

A. Tchamova¹, T. Semerdjiev², P. Konstantinova³, Jean Dezert⁴

^{1,2,3}Institute for Parallel Processing, Bulgarian Academy of Sciences, “Acad. G. Bonchev”
Str.,bl.25-A, 1113, Sofia Bulgaria

⁴ONERA, 29 Av. de la Division Leclerc 92320, Chatillon, France

Generalized Data Association for Multitarget Tracking in Clutter

Published in:

Florentin Smarandache & Jean Dezert (Editors)

Advances and Applications of DSMT for Information Fusion

(Collected works), Vol. I

American Research Press, Rehoboth, 2004

ISBN: 1-931233-82-9

Chapter XIV, pp. 303 - 324

Abstract: *The objective of this chapter is to present an approach for target tracking in cluttered environment, which incorporates the advanced concept of generalized data (kinematics and attribute) association (GDA) to improve track maintenance performance in complicated situations (closely spaced and/or crossing targets), when kinematics data are insufficient for correct decision making. It uses Global Nearest Neighbour-like approach and Munkres algorithm to resolve the generalized association matrix. The main peculiarity consists in applying the principles of Dezert-Smarandache theory (DSmT) of plausible and paradoxical reasoning to model and process the utilized attribute data. The new general Dezert-Smarandache hybrid rule of combination is used to deal with particular integrity constraints associated with some elements of the free distributive lattice. The aim of the performed study is to provide coherent decision making process related to generalized data association and to improve the overall tracking performance. A comparison with the corresponding results, obtained via Dempster-Shafer theory is made.*

This work has been partially supported by MONT grants I-1205/02, I-1202/02 and by Center of Excellence BIS21 grant ICA1-2000-70016

14.1 Introduction

One important function of each radar surveillance system in cluttered environment is to keep and improve targets' tracks maintenance performance. It becomes a crucial and challenging problem especially in complicated situations of closely spaced, and/or crossing targets. The design of a modern multitarget tracking (MTT) algorithms in a such real-life stressful environment motivates the incorporation of the advanced concepts for generalized data association. In order to resolve correlation ambiguities and to select the best observation-track pairings, in this study, a particular generalized data association (GDA) approach is proposed and incorporated in a MTT algorithm. It allows the introduction of target attribute into the association logic, based on the general Dezert-Smarandache rule for combination, which is adapted to deal with possible integrity constraints on the problem under consideration due to the true nature of the elements involved into it. This chapter extends recent research work published in [15] which was limited to target tracking in clutter-free environment.

14.2 Basic Elements of Tracking Process

The tracking process consists of two basic elements: *data association* and *track filtering*. The first element is often considered as the most important. Its goal is to associate observations to existing tracks.

14.2.1 Data Association

To eliminate unlikely observation-to-track pairing at the beginning a validation region (gate) is formed around the predicted track position. The measurements in the gate are candidates for association to the corresponding track.

14.2.1.1 Gating

We assume zero-mean Gaussian white noise for measurements. The vector difference between received measurement vector $\mathbf{z}_j(k)$ and predicted measurement vector $\hat{\mathbf{z}}_i(k|k-1)$ of target i is defined to be residual vector (called innovation)

$$\tilde{\mathbf{z}}_{ij}(k) = \mathbf{z}_j(k) - \hat{\mathbf{z}}_i(k|k-1)$$

with residual covariance matrix $\mathbf{S} = \mathbf{H}\mathbf{P}\mathbf{H}' + \mathbf{R}$, where \mathbf{P} is the state prediction covariance matrix, \mathbf{H} is the measurement matrix and \mathbf{R} is the measurement covariance matrix [2, 3, 4, 5]. The scan indexes k will be dropped for notational convenience. The norm (normalized distance function) of the innovation is evaluated as:

$$d_{ij}^2 = \tilde{\mathbf{z}}_{ij}' \mathbf{S}^{-1} \tilde{\mathbf{z}}_{ij}$$

One defines a threshold constant for gate γ such that correlation is allowed if the following relationship is satisfied

$$d_{ij}^2 \leq \gamma \quad (14.1)$$

Assume that the measurement vector size is M . The quantity d_{ij}^2 is the sum of the squares of M independent Gaussian random variables with zero means and unit standard deviations. For that reason d_{ij}^2 will have χ_M^2 distribution with M degrees of freedom and allowable probability of a valid observation falling outside the gate. The threshold constant γ can be defined from the table of the chi-square (χ_M^2) distribution [3].

14.2.1.2 Generalized Data Association (GDA)

If a single observation is within a gate and if that observation is not within a gate of any other track, the observation can be associated with this track and used to update the track filter. But in a dense target environment additional logic is required when an observation falls within the gates of multiple target tracks or when multiple observations fall within the gate of a target track.

When attribute data are available, the generalized probability can be used to improve the assignment. In view of independence of the kinematic and attribute measurement errors, the generalized probability for measurement j originating from track i is:

$$P_{\text{gen}}(i, j) = P_{\text{k}}(i, j)P_{\text{a}}(i, j)$$

where $P_{\text{k}}(i, j)$ and $P_{\text{a}}(i, j)$ are kinematic and attribute probability terms respectively.

Our goal is to choose a set of assignments $\{\chi_{ij}\}$, for $i = 1, \dots, n$ and $j = 1, \dots, m$, that assures maximum of the total generalized probability sum. To find it, we use the solution of the assignment problem

$$\min \sum_{i=1}^n \sum_{j=1}^m a_{ij} \chi_{ij}$$

where:

$$\chi_{ij} = \begin{cases} 1 & \text{if measurement } j \text{ is assigned to track } i \text{ according to assignment problem solution} \\ 0 & \text{otherwise} \end{cases}$$

If, in the attempt to maximize the number of assignments, the assignment algorithm chooses a pairing that does not satisfy the gate, the assignment is later removed.

Because our probabilities vary $0 \leq P_{\text{k}}(i, j), P_{\text{a}}(i, j) \leq 1$ and to satisfy the condition to be minimized, the elements of the particular assignment matrix are defined as :

$$a_{ij} = 1 - P_{\text{gen}}(i, j) = 1 - P_{\text{k}}(i, j)P_{\text{a}}(i, j)$$

14.2.2 Filtering

The used tracking filter is the first order extended Kalman filter [7] for *target state vector* $\mathbf{x} = [x \dot{x} y \dot{y}]'$, where x and y are Cartesian coordinates and \dot{x} and \dot{y} are velocities along Cartesian axes and *measurement vector* $\mathbf{z} = [\beta D]'$, where β is the azimuth (measured from the North), and D is the distance from the observer to the target under consideration.

The measurement function $\mathbf{h}(\cdot)$ is (assuming the sensor located at position (0,0)):

$$\mathbf{h}(\mathbf{x}) = [h_1(\mathbf{x}) \ h_2(\mathbf{x})]' = [\arctan(\frac{x}{y}) \ \sqrt{x^2 + y^2}]'$$

and the Jacobian [3]:

$$\mathbf{H} = [H_{ij}] = [\partial h_i / \partial x_j] \quad i = 1, 2 \quad j = 1, \dots, 4$$

We assume constant velocity target model. The process noise covariance matrix is: $\mathbf{Q} = \sigma_v^2 \mathbf{Q}_T$, where T is the sampling/scanning period, σ_v is standard deviation of the process noise and \mathbf{Q}_T is given by [8]:

$$\mathbf{Q}_T = \text{diag}(\mathbf{Q}_{2 \times 2}, \mathbf{Q}_{2 \times 2}) \quad \text{with} \quad \mathbf{Q}_{2 \times 2} = \begin{bmatrix} T^4 & T^3 \\ 4 & 2 \\ T^3 & T^2 \\ 2 & T^2 \end{bmatrix}$$

The measurement error matrix is $\mathbf{R} = \text{diag}(\sigma_\beta^2, \sigma_D^2)$ where σ_β and σ_D are the standard deviations of measurement errors for azimuth and distance.

The track initiation is performed by two-point differencing [7]. After receiving observations for first two scans the initial state vector is estimated by $\hat{\mathbf{x}} = [x(2) \ \frac{x(2)-x(1)}{T} \ y(2) \ \frac{y(2)-y(1)}{T}]'$ where $(x(1), y(1))$ and $(x(2), y(2))$ are respectively the target positions at the first scan for time stamp $k = 1$, and at the second scan for $k = 2$. The initial (starting at time stamp $k = 2$) state covariance matrix \mathbf{P} is evaluated by:

$$\mathbf{P} = \text{diag}(\mathbf{P}_{2 \times 2}^x, \mathbf{P}_{2 \times 2}^y) \quad \text{with} \quad \mathbf{P}_{2 \times 2}^{(\cdot)} = \begin{bmatrix} \sigma_{(\cdot)}^2 & \sigma_{(\cdot)}^2 \\ \sigma_{(\cdot)}^2 & T \\ \sigma_{(\cdot)}^2 & 2\sigma_{(\cdot)}^2 \\ T & T^2 \end{bmatrix}$$

where the index (\cdot) must be replaced by either x or y indexes with $\sigma_x^2 \approx \sigma_D^2 \sin^2(z_\beta) + z_D^2 \sigma_\beta^2 \cos^2(z_\beta)$ and $\sigma_y^2 \approx \sigma_D^2 \cos^2(z_\beta) + z_D^2 \sigma_\beta^2 \sin^2(z_\beta)$. z_β and z_D are the components of the measurement vector received at scan $k = 2$, i.e. $\mathbf{z} = [z_\beta \ z_D]'$ = $\mathbf{h}(\mathbf{x}) + \mathbf{w}$ with $\mathbf{w} \sim \mathcal{N}(\mathbf{0}, \mathbf{R})$.

14.3 The Attribute Contribution to GDA

Data association with its goal of partitioning observations into tracks is a key function of any surveillance system. An advanced tendency is the incorporation of generalized data (kinematics and attribute) association to improve track maintenance performance in complicated situations, when kinematics data are insufficient for coherent decision making process. Analogously with the kinematic tracking, the attribute

tracking can be considered as the process of combining information collected over time from one or more sensors to refine the knowledge about the evolving attributes of the targets. The motivation for attribute fusion is inspired from the necessity to ascertain the targets' types, information, that in consequence has an important implication to enhance the tracking performance. A number of techniques, probabilistic in nature are available for attribute fusion. Their analysis led us to belief, that the theory of Dempster-Shafer is well suited for representing uncertainty, but especially in case of low conflicts between the bodies of evidence. When the conflict increases and becomes high, (case, which often occurs in data association process) the combinational rule of Dempster hides the risk to produce indefiniteness. To avoid that significant risk we consider the form of attribute likelihood function within the context of DS_m theory, i.e. the term to be used for computing the probabilities of validity for data association hypotheses. There are a few basic steps, realizing the concept of attribute data association.

14.3.1 The Input Fuzzification Interface

Fuzzification interface (see fig. 14.1) transforms numerical measurement received from a sensor into fuzzy set in accordance with the a priori defined fuzzy partition of input space-the frame of discernments Θ . This frame includes all considered linguistic values related to the chosen particular input variable and their corresponding membership functions. The fuzzification of numerical sensory data needs dividing an optimal membership into a suitable number of fuzzy sets [14]. Such division provides smooth transitions and overlaps among the associated fuzzy sets, according to the particular real world situation.

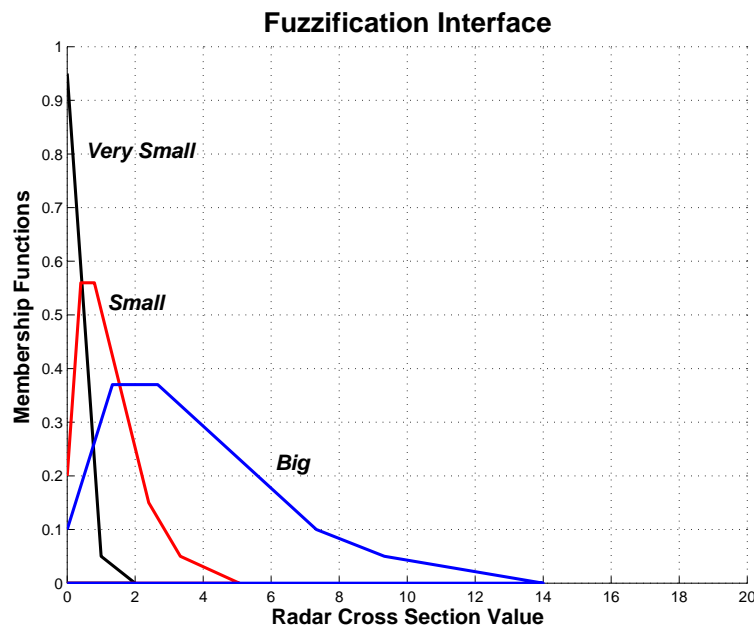


Figure 14.1: Fuzzification interface

The considerable input variable in the particular case is the Radar Cross Section (RCS) of the observed targets. In our work the modeled RCS data are analyzed to determine the target size with the subsequent declaration that the observed target is an aircraft of specified type (Fighter, Cargo) or False Alarms. Taking it in mind, we define two frames of discernments: first one according to the **size of RCS**: $\Theta_1 = \{\text{Very Small (VS), Small (S), Big (B)}\}$ and the second one determining the corresponding to its **Target Type** $\Theta_2 = \{\text{False Alarms (FA), Fighter (F), Cargo (C)}\}$.

The radar cross section according to the real targets is modeled as Swerling 3 type, where the density function for the RCS σ is given by:

$$f(\sigma) = \frac{4\sigma}{\sigma_{\text{ave}}^2} \exp\left[-\frac{2\sigma}{\sigma_{\text{ave}}}\right]$$

with the average RCS (σ_{ave}) varying between different targets' types [16]. The cumulative distribution function of the radar cross section is given by

$$F(\sigma_0) = P\{0 \leq \sigma \leq \sigma_0\} = 1 - \left(1 + \frac{2\sigma_0}{\sigma_{\text{ave}}}\right) \exp\left[-\frac{2\sigma_0}{\sigma_{\text{ave}}}\right]$$

Since the probabilities $F(\sigma_0)$ for having different values of radar cross section are uniformly distributed in the interval $[0, 1]$ over time (i.e. these values are uncorrelated in time), a sample of observation of the RCS can be simulated by solving equation:

$$\left(1 + \frac{2\sigma_0}{\sigma_{\text{ave}}}\right) \exp\left[-\frac{2\sigma_0}{\sigma_{\text{ave}}}\right] = 1 - x$$

where x is a random number that is uniformly distributed between 0 and 1.

The scenario considered in our work deals with targets' types Fighter (F) and Military Cargo (C) with an average RCS :

$$\sigma_{\text{ave}}^{\text{F}} = 1.2 m^2 \quad \text{and} \quad \sigma_{\text{ave}}^{\text{C}} = 4 m^2$$

The radar cross section according to the False Alarms [1] is modeled as Swerling 2 type, where the density function for the RCS is given by:

$$f(\sigma) = \frac{1}{\sigma_{\text{ave}}} \exp\left[-\frac{\sigma}{\sigma_{\text{ave}}}\right] \quad \text{with} \quad \sigma_{\text{ave}} = 0.3 m^2$$

The cumulative distribution function is given by

$$F(\sigma_0) = P\{0 \leq \sigma \leq \sigma_0\} = 1 - \exp\left[-\frac{\sigma_0}{\sigma_{\text{ave}}}\right]$$

A sample of observation of the RCS can be computed by solving equation:

$$\exp\left[-\frac{\sigma_0}{\sigma_{\text{ave}}}\right] = 1 - x$$

where x is a random number that is uniformly distributed between 0 and 1.

The input fuzzification interface maps the current modeled RCS values into three fuzzy sets: **VerySmall**, **Small** and **Big**, which define the corresponding linguistic values, defining the variable "RCS". Their membership functions are not arbitrarily chosen, but rely on the calculated respective histograms for 10000 Monte Carlo runs. Actually these fuzzy sets form the frame of discernments Θ_1 . After fuzzification the new RCS value (rcs) is obtained in the form :

$$\text{rcs} \Rightarrow [\mu_{\text{VerySmall}}(\text{rcs}), \mu_{\text{Small}}(\text{rcs}), \mu_{\text{Big}}(\text{rcs})]$$

In general, the grades $\mu_{\text{VerySmall}}(\text{rcs})$, $\mu_{\text{Small}}(\text{rcs})$, $\mu_{\text{Big}}(\text{rcs})$ represent the possibilities the new RCS value to belong to the elements of the frame Θ_1 and there is no requirement to sum up to unity. Figure 14.2 below shows the way which the new observations for Cargo, Fighter and False Alarms are modeled for 500 Monte Carlo runs, using the corresponding Swerling type functions type 3 and 2. It is evident that they are too much mixed. It influences over the distinction between them. That fact hides the possibility of intrinsic conflicts between the fused bodies of evidence (general basic belief assignment (gbba) of targets' tracks and observations), because of their imprecise belief functions and consequently yields a poor targets tracks' performance. To deal successfully with such kind of stressful, but real situation, we need DSsm theory to process flexibly and adequately these conflicts.

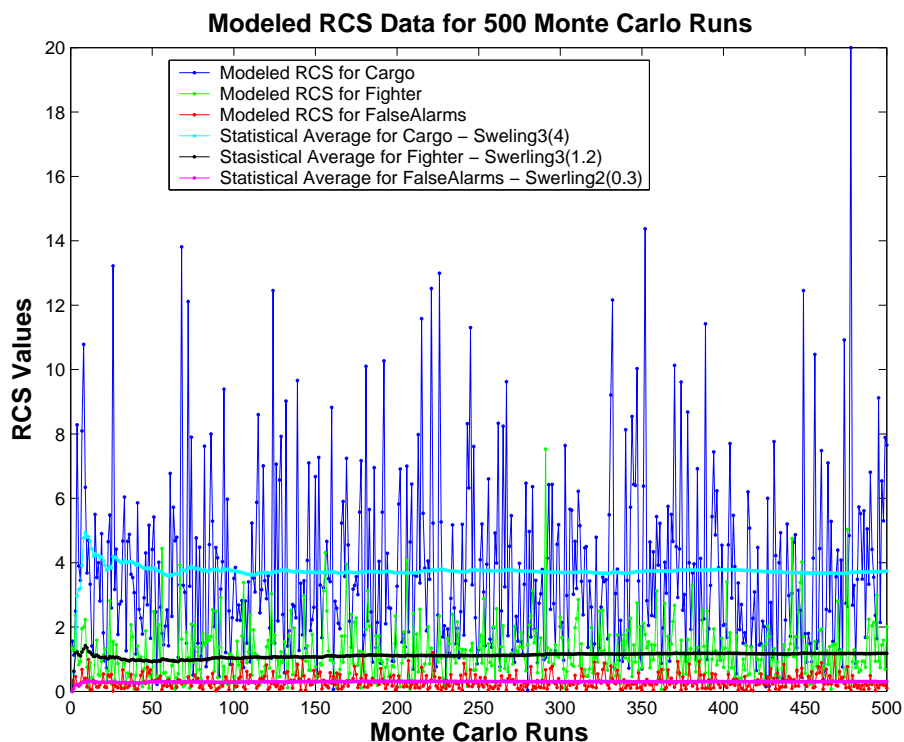


Figure 14.2: Simulation of RCS values over 500 Monte Carlo runs

14.3.2 Tracks' Updating Procedures

14.3.2.1 Using Classical DS_m Combinational Rule

After receiving the new observations, detected during the current scan k , to obey the requirements to guarantee that their particular belief assignment $m(\cdot)$ are general information granules, it is necessary to transform each measurement's set of fuzzy membership grades into the corresponding mass function, before being fused. It is realized through normalization with respect to the unity:

$$m_{\text{meas}}(C) = \frac{\mu_C(\text{rcs})}{\sum_{C \in \Theta_1} \mu_C(\text{rcs})}, \quad \forall C \in \Theta_1 = \{\text{VS}, \text{S}, \text{B}\}$$

The general basic belief assignments (gbba) of tracks' histories are described in terms of the hyper-power set :

$$\begin{aligned} D^{\Theta_1} = \{ & \emptyset, \text{VS}, \text{S}, \text{B}, \text{VS} \cap \text{S} \cap \text{B}, \text{VS} \cap \text{S}, \text{VS} \cap \text{B}, \text{S} \cap \text{B}, (\text{VS} \cup \text{S}) \cap \text{B}, (\text{VS} \cup \text{B}) \cap \text{S}, \\ & (\text{S} \cup \text{B}) \cap \text{VS}, (\text{VS} \cap \text{S}) \cup (\text{VS} \cap \text{B}) \cup (\text{S} \cap \text{B}), (\text{VS} \cap \text{S}) \cup \text{B}, (\text{VS} \cap \text{B}) \cup \text{S}, \\ & (\text{S} \cap \text{B}) \cup \text{VS}, \text{VS} \cup \text{S}, \text{VS} \cup \text{B}, \text{S} \cup \text{B}, \text{VS} \cup \text{S} \cup \text{B} \} \end{aligned}$$

Then DS_m classical combinational rule (see chapter 1) is used for tracks' updating:

$$m_{\text{upd}}^{ij}(C) = [m_{\text{hist}}^i \oplus m_{\text{meas}}^j](C) = \sum_{A, B \in D^{\Theta_1}, A \cap B = C} m_{\text{hist}}^i(A) m_{\text{meas}}^j(B)$$

where $m_{\text{upd}}^{ij}(\cdot)$ represents the gbba of the updated track i with the new observation j ; m_{hist}^i , m_{meas}^j are respectively gbba vectors of track's i history and the new observation j .

It is important to note, that for us the two considered independent sources of information are the tracks' histories and the new observations with their gbbas maintained in terms of the two hyper-power sets. That way we assure to obtain and to keep the decisions according to the target types during all the scans.

Since, DS_mT uses a frame of discernment, which is exhaustive, but in general case not exclusive, we are able to take into account and to utilize the paradoxical information $\text{VS} \cap \text{S} \cap \text{B}$, $\text{VS} \cap \text{S}$, $\text{VS} \cap \text{B}$ and $\text{S} \cap \text{B}$. This information relates to the cases, when the RCS value resides in an overlapping regions, when it is hard to make proper judgement about the tendency of behavior of its value. Actually these nonempty sets and related to it mass assignments contribute to a better understanding of the overall tracking process.

14.3.2.2 Using Hybrid DS_m Combinational Rule

As it was mentioned above in our work, RCS data here are used to analyze and subsequently to determine the specified type of the observed targets. Because of this it is maintained the second frame of

discernement $\Theta_2 = \{\text{False Alarm (FA)}, \text{Fighter (F)}, \text{Cargo (C)}\}$, in terms of which the decisions according to target types have to be made. Doing this, we take in mind the following correspondencies:

- If rcs is **Very Small** then the "target" is **False Alarm**
- If rcs is **Small** then the target is **Fighter**
- If rcs is **Big** then the target is **Cargo**

We may transform the gbba of updated tracks, formed in D^{Θ_1} into respective gbba in D^{Θ_2} , i.e:

$$m_{\text{upd}}^{ij}(C_{C \in D^{\Theta_2}}) = m_{\text{upd}}^{ij}(C_{C \in D^{\Theta_1}})$$

But let us go deeper into the meaning of the propositions in the second hyper-power set. It should be:

$$\begin{aligned} D^{\Theta_2} = \{ & \emptyset, \text{FA}, \text{F}, \text{C}, \text{FA} \cap \text{F} \cap \text{C}, \text{FA} \cap \text{F}, \text{FA} \cap \text{C}, \text{F} \cap \text{C}, (\text{FA} \cup \text{F}) \cap \text{C}, (\text{FA} \cup \text{C}) \cap \text{F}, \\ & (\text{F} \cup \text{C}) \cap \text{FA}, (\text{FA} \cap \text{F}) \cup (\text{FA} \cap \text{C}) \cup (\text{F} \cap \text{C}), (\text{FA} \cap \text{F}) \cup \text{C}, (\text{FA} \cap \text{C}) \cup \text{F}, \\ & (\text{F} \cap \text{C}) \cup \text{FA}, \text{FA} \cup \text{F}, \text{FA} \cup \text{C}, \text{F} \cup \text{C}, \text{FA} \cup \text{F} \cup \text{C} \} \end{aligned}$$

In the real life however, it is a proven fact, that the target can not be in one and the same time FalseAlarm and Fighter; FalseAlarm and Cargo; Fighter and Cargo; FalseAlarm and Fighter and Cargo. It leads to the following hybrid DSm model $\mathcal{M}_1(\Theta_2)$, built by introducing the following exclusivity constraints (see chapter 4 for a detailed presentation of the hybrid DSm models and the hybrid DSm rule of combination):

$$\text{FA} \cap \text{F} \stackrel{\mathcal{M}_1}{\equiv} \emptyset \quad \text{FA} \cap \text{C} \stackrel{\mathcal{M}_1}{\equiv} \emptyset \quad \text{F} \cap \text{C} \stackrel{\mathcal{M}_1}{\equiv} \emptyset \quad \text{FA} \cap \text{F} \cap \text{C} \stackrel{\mathcal{M}_1}{\equiv} \emptyset$$

These exclusivity constraints imply directly the following ones:

$$\begin{aligned} (\text{FA} \cup \text{F}) \cap \text{C} & \stackrel{\mathcal{M}_1}{\equiv} \emptyset & (\text{FA} \cap \text{F}) \cup \text{C} & \stackrel{\mathcal{M}_1}{\equiv} \text{C} \\ (\text{FA} \cup \text{C}) \cap \text{F} & \stackrel{\mathcal{M}_1}{\equiv} \emptyset & (\text{FA} \cap \text{C}) \cup \text{F} & \stackrel{\mathcal{M}_1}{\equiv} \text{F} \\ (\text{F} \cup \text{C}) \cap \text{FA} & \stackrel{\mathcal{M}_1}{\equiv} \emptyset & (\text{F} \cap \text{C}) \cup \text{FA} & \stackrel{\mathcal{M}_1}{\equiv} \text{FA} \end{aligned}$$

and also the more generalized one

$$(\text{FA} \cap \text{F}) \cup (\text{FA} \cap \text{C}) \cup (\text{F} \cap \text{C}) \stackrel{\mathcal{M}_1}{\equiv} \emptyset$$

The obtained that way model corresponds actually to Shafer's model, which can be considered as a particular case of the generalized free DSm model.

Therefore, while the corresponding sets in D^{Θ_1} are usually non empty, because of the exclusivity constraints, in the second frame Θ_2 , the hyper-power set D^{Θ_2} is reduced to classical power set :

$$D_{\mathcal{M}_1}^{\Theta_2} = \{\emptyset, FA, F, C, FA \cup F, FA \cup C, F \cup C, FA \cup F \cup C\}$$

So, we have to update the previous fusion result, obtained via the classical DS_m rule of combination with this new information on the model $\mathcal{M}_1(\Theta_2)$ of the considered problem. It is solved with the hybrid DS_m rule (see chapter 4), which transfers the mass of these empty sets to the non-empty sets of $D_{\mathcal{M}_1}^{\Theta_2}$.

14.4 The Generalized Data Association Algorithm

We consider a particular cluster and assume the existence of a set of n tracks at the current scan and a set of m received observations. A validated measurement is one which is either inside or on the boundary of the validation gate of a target. The inequality given in (14.1) is a validation test. It is used for filling the assignment matrix \mathbf{A} :

$$\mathbf{A} = [A_{ij}] = \begin{bmatrix} a_{11} & a_{12} & a_{13} & \vdots & a_{1m} \\ a_{21} & a_{22} & a_{23} & \vdots & a_{2m} \\ \vdots & \vdots & \vdots & \vdots & \vdots \\ a_{n1} & a_{n2} & a_{n3} & \vdots & a_{nm} \end{bmatrix}$$

The elements of the assignment matrix \mathbf{A} have the following values [13]:

$$a_{ij} = \begin{cases} \infty & \text{if } d_{ij}^2 > \gamma \\ 1 - P_k(i, j)P_a(i, j) & \text{if } d_{ij}^2 \leq \gamma \end{cases}$$

The solution of the assignment matrix is the one that minimizes the sum of the chosen elements. We solve the assignment problem by realizing the extension of Munkres algorithm, given in [10]. As a result, it obtains the optimal measurements to tracks association. Because of the considered crossing and/or closely spaced target scenarios, to produce the probability terms P_k and P_a , the joint probabilistic approach is used [7]. It assures a common base for their defining, making that way them to be compatible. The joint probabilistic data association (JPDA) approach imposes restriction on the problem size because of exponential increasing of the number of generated hypotheses and the time for assignment problem solution. That's why it is advisable to make clustering before solving data association problem. Cluster is a set of closely spaced objects. In our case if two tracks have an observation in their overlapping parts of the gates, the tracks form cluster i.e. their clusters are merged. In such a way the number of clusters are equal or less than the number of tracked tracks. The clustering is usefull at least for two reasons:

1. In such a way the size of assignment matrix and also the time for its solution decreases;
2. The number of hypotheses for JPDA like approach for defining kinematic and attribute probabilities also decreases.

In the worst case when all m measurements fall in the intersection of the validation regions of all n tracks, the number of hypotheses can be obtained as:

$$S(n, m) = \sum_{i=0}^{\min(n, m)} C_m^i A_n^i$$

where

$$C_m^i \triangleq \frac{m!}{i!(m-i)!} \text{ for } 0 \leq i \leq m \quad \text{and} \quad A_n^i \triangleq \frac{n!}{(n-i)!} \text{ for } 0 \leq i \leq n$$

With these formulae the number of hypotheses for various values of the m and n are computed and are shown in the following table. The enormous increasing of the number of hypothesis can be seen.

	Hyp. #		Hyp. #		Hyp. #
$n = 2, m = 2$	7	$n = 4, m = 4$	209	$n = 6, m = 6$	13327
$n = 2, m = 3$	13	$n = 4, m = 5$	501	$n = 7, m = 8$	394353
$n = 3, m = 3$	34	$n = 5, m = 5$	1546	$n = 10, m = 9$	58941091
$n = 3, m = 4$	73	$n = 5, m = 6$	4051	$n = 10, m = 10$	234662231

Table 14.1: Worst case hypotheses number

As further improvement, first k -best hypotheses can be used [12] as the score of the hypotheses decrease and a big amount of hypotheses practically does not influence the result. Another original frame of hypotheses generation has been considerably optimized in [9] and that way it becomes a practical alternative of Murty's approach.

To define the probabilities for data association for different scenarios with random number of false alarms we implement the following steps on each scan:

1. **Check gating** - using information for the received observations and for tracked targets (at the moment) and for each pair (track i - observation j) check inequality (14.1). As a result an array presents each observation in which track's gates is fallen.
2. **Clustering** - define clusters with tracks and observations fallen in their gates.
3. **For each cluster:**

3.1 - Generate hypotheses following Depth First Search (DFS) procedure with certain constraints [17]. In the JPDAF approach, the two constraints which have to be satisfied for a feasible event are:

- (a) each observation can have only one origin (either a specific target or clutter), and

(b) no more than one observation originates from a target.

As a result of hypotheses generation for each hypothesis is defined a set of numbers representing the observations assigned to the corresponding tracks, where the zero represents the assignment of no observation to a given track.

3.2 - Compute hypothesis probabilities for kinematic and attribute contributions (detailed in the next paragraphs).

3.3 - Fill assignment matrix, solve assignment problem and define observation to track association.

14.4.1 Kinematics probability term for generalized data association

On the basis of defined hypotheses, the kinematic probabilities are computed as:

$$P'(H_l) = \beta^{N_M - (N_T - N_{nD})} (1 - P_d)^{N_{nD}} P_d^{(N_T - N_{nD})} \prod_{i \neq 0, j \neq 0 | (i,j) \in H_l} g_{ij}$$

N_M being the number of observations in cluster, N_T the number of targets, N_{nD} the number of not detected targets. $(i, j) \in H_l$ involved in the product represents all the possible observation to track associations involved in hypothesis H_l . The likelihood function g_{ij} , associated with the assignment of observation j to track i is:

$$g_{ij} = \frac{e^{-d_{ij}^2/2}}{(2\pi)^{M/2} \sqrt{|\mathbf{S}_i|}}$$

P_d is the probability of detection and β is the extraneous return density, that includes probability density for new tracks and false alarms:

$$\beta = \beta_{NT} + \beta_{FA}$$

The normalized probabilities are computed as:

$$P_k(H_l) = \frac{P'(H_l)}{\sum_{k=1}^{N_H} P'(H_k)}$$

where N_H is the number of hypotheses. To compute the probability $P_k(i, j)$ that observation j should be assigned to track i , a sum is taken over the probabilities $P_k(\cdot)$ from those hypotheses H_l , in which this assignment occurs.

As an particular example for a cluster with two tracks and two new observations, see Fig. 14.3, detected during the moment of their closely spaced movement, where $P1$ and $P2$ are the tracks' predictions and $O1$, $O2$ are the received observations. The table 14.2 shows the particular hypotheses for the alternatives with respect to targets tracks and associated probabilities.

Hyp. #	Track 1	Track 2	Hyp. proba. $P'(H_l)$
H_1	0	0	$(1 - P_d)^2 \beta^2$
H_2	1	0	$g_{11} P_d (1 - P_d) \beta$
H_3	2	0	$g_{12} P_d (1 - P_d) \beta$
H_4	0	1	$g_{21} P_d (1 - P_d) \beta$
H_5	0	2	$g_{22} P_d (1 - P_d) \beta$
H_6	1	2	$g_{11} g_{22} P_d^2$
H_7	2	1	$g_{12} g_{21} P_d^2$

Table 14.2: Target-oriented hypothesis based on kinematics.

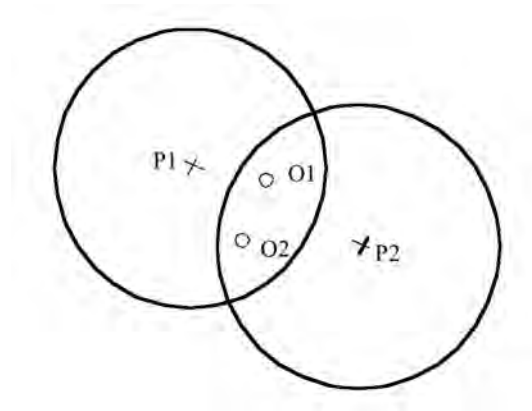


Figure 14.3: Scenario with two tracks and two observations

14.4.2 Attribute probability terms for generalized data association

The way of calculating the attribute probability term follows the joint probabilistic approach.

$$P''(H_l) = \prod_{i \neq 0, j \neq 0 | (i,j) \in H_l} d_e(i, j)$$

where

$$d_e(i, j) = \sqrt{\sum_{C \in D^{\Theta_1}} [m_{\text{hist}}^i(C) - m_{\text{CandHist}}^{i,j}(C)]^2}$$

where $m_{\text{CandHist}}^{i,j}(C)$ is a candidate history of the track - result, obtained after the fusion via DSsm classical rule of combination between the new received attribute observation j and predicted track's attribute state of the track i (the confirmed track history from the previous scan).

In the case of existence of two tracks and two new observations, considered in previous section and on the basis of the hypotheses matrix, one can obtain the probabilities of the hypotheses according to the following table:

Hyp. #	Track 1	Track 2	Closeness measure
H_1	0	0	$P''(H_1) = d_e(0, 0) = 0$
H_2	1	0	$P''(H_2) = d_e(1, 1)$
H_3	2	0	$P''(H_3) = d_e(1, 2)$
H_4	0	1	$P''(H_4) = d_e(2, 1)$
H_5	0	2	$P''(H_5) = d_e(2, 2)$
H_6	1	2	$P''(H_6) = d_e(1, 1)d_e(2, 2)$
H_7	2	1	$P''(H_7) = d_e(1, 2)d_e(2, 1)$

Table 14.3: Target-oriented hypothesis based on attributes.

The corresponding normalized probabilities of association drawn from attribute information are obtained as:

$$P_a(H_l) = \frac{P''(H_l)}{\sum_{k=1}^{N_H} P''(H_k)}$$

where N_H is the number of association hypotheses.

To compute the probability $P'_a(i, j)$ that observation j should be assigned to track i , a sum is taken over the probabilities $P_a(\cdot)$ from those hypotheses H_l , in which this assignment occurs. Because the Euclidean distance is inversely proportional to the probability of association, the probability term $P_a(i, j) = 1 - P'_a(i, j)$ is used to match the corresponding kinematics probability.

14.5 Simulation scenarios

14.5.1 Simulation scenario1: Crossing targets

The simulation scenario consists of two air targets (Fighter and Cargo) and a stationary sensor at the origin with $T_{\text{scan}} = 5$ sec., measurement standard deviations 0.3 deg and 60 m for azimuth and range respectively. The targets movement is from West to East with constant velocity of 250 m/sec. The headings of the fighter and cargo are 225 deg and 315 deg from North respectively. During the scan 11th-14th the targets perform maneuvers with 2.5g. Their trajectories are closely spaced in the vicinity of the two crossing points. The target detection probabilities have been set to 0.99 for both targets and the extraneous return density β to 10^{-6} . In our scenario we consider the more complicated situations, when the false alarms are available. The number of false alarms are Poisson distributed and their positions are uniformly distributed in the observation space.

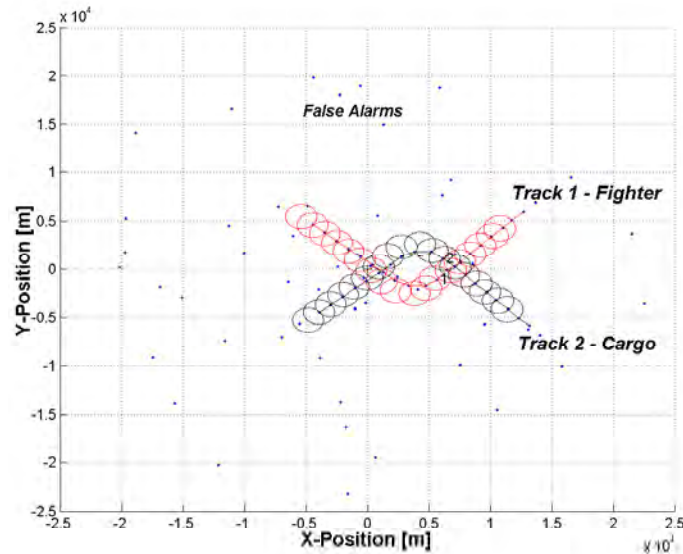


Figure 14.4: Typical simulation for scenario 1 - Two Crossing Targets' Tracks

14.5.2 Simulation scenario 2: Closely spaced targets

The second simulation scenario is influenced by the recent works of Bar-Shalom, Kirubarajan and Gokberk [6], which considers a case of closely spaced ground targets, moving in parallel. Our case consists of four air targets (alternating Fighter,Cargo, Fighter,Cargo) moving with constant velocity of 100 m/sec. The heading at the beginning is 155 [deg] from North. The targets make maneuvers with 0.85g - (right, left , right turns). The sensor parameters and the false alarms are the same as in the first scenario.

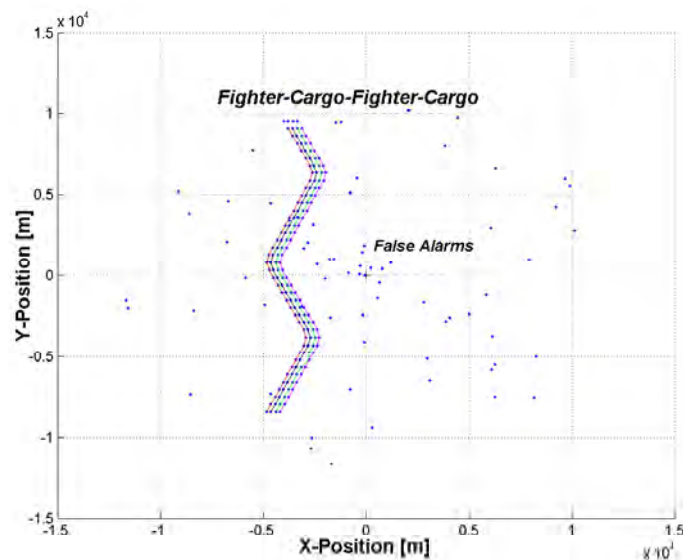


Figure 14.5: Typical simulation for scenario 2 - Four Closely Spaced Air Targets' Tracks

14.6 Simulation results

In this section the obtained simulation results, based on 100 Monte Carlo runs are presented. The goal is to demonstrate how the attribute measurements contribute for the improvement of the track performance, especially in critical cases, when the tracks are crossing and/or closely spaced.

14.6.1 Simulation results: Two crossing targets

In the case when only kinematics data are available for data association (see fig. 14.6), it is evident that after scan 15 (the second crossing moment for the targets), the tracking algorithm loses the proper targets' direction.

Here the *Tracks' Purity* performance criterion is used to examine the ratio of the right associations. Track purity is considered as a ratio of the number of correct observation-target associations (in case of detected target) over the total number of available observations during tracking scenario.

The results from table 14.4 show the proper (observation-track) associations in that case. Here "missed" is used for the case when in the track's gate there is no observation, and "FA" is used for the case, when the track is associated with the false alarm.

	Obs. 1	Obs. 2	Missed	FA
Track 1	0.7313	0.2270	0.0304	0.0113
Track 2	0.2409	0.7035	0.0426	0.0130

Table 14.4: Tracks' Purity in case of Kinematics Only Data Association (KODA).

Table 14.5 shows the result, when attribute data are utilized in the generalized data association algorithm in order to improve the tracks' maintenance performance. The hybrid DS_m rule is applied to produce the attribute probability term in generalized assignment matrix. As a result it is obvious that the tracks' purity increases

	Obs. 1	Obs. 2	Missed	FA
Track 1	0.8252	0.1496	0.0165	0.0087
Track 2	0.1557	0.8243	0.0165	0.0035

Table 14.5: Tracks' Purity in case of Generalized Data Association based on DS_mT.

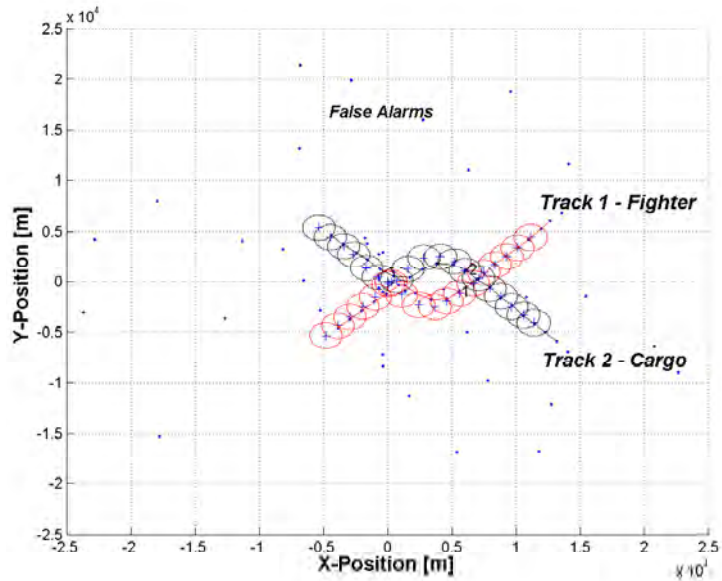


Figure 14.6: Performance of Tracking Algorithm with Kinematics Only Data Association

14.6.2 Simulation results: Four closely spaced targets

Figure 14.7 shows the performance of the implemented tracking algorithm with kinematics only data association. One can see that the four closely spaced moving in parallel targets lose the proper directions and the tracks switch.

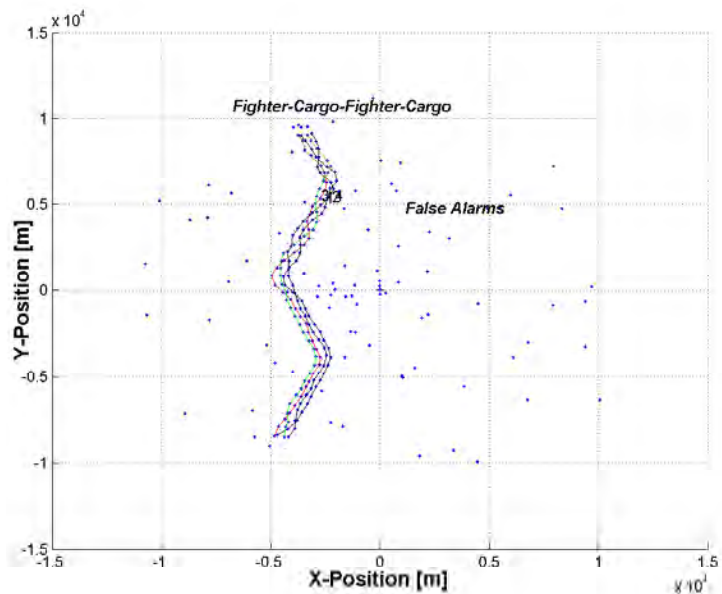


Figure 14.7: Performance of Tracking Algorithm with Kinematics Only Data Association

The results in table 14.6 show the proper (observation-track) associations in that case. The corresponding results in case of GDA based on DSmT are described in table 14.7.

	Obs. 1	Obs. 2	Obs. 3	Obs. 4	Missed	FA
Track 1	0.5874	0.3321	0.0558	0.0216	0.0021	0.0011
Track 2	0.2895	0.5411	0.1126	0.0521	0.0021	0.0026
Track 3	0.1089	0.0874	0.5084	0.2916	0.0021	0.0016
Track 4	0.0126	0.0332	0.3168	0.6337	0.0005	0.0032

Table 14.6: Tracks' Purity in case of Kinematics Only Data Association.

	Obs. 1	Obs. 2	Obs. 3	Obs. 4	Missed	FA
Track 1	0.7026	0.2437	0.0037	0.0216	0.0026	0.0005
Track 2	0.2253	0.5826	0.0584	0.0521	0.0016	0.0000
Track 3	0.0511	0.0853	0.6047	0.2563	0.0011	0.0016
Track 4	0.0189	0.0853	0.2121	0.6805	0.0016	0.0016

Table 14.7: Tracks' Purity with GDA based on DSmT.

14.6.3 Simulation results of GDA based on Dempster-Shafer theory

The results based on Dempster-Shafer theory for attribute data association are described in the tables below. For scenario 1 (**two crossing targets**), the tracks' purity is obtained in table 14.8. For scenario 2 (**four closely spaced targets**), the tracks' purity performance is obtained in table 14.9.

	Obs. 1	Obs. 2	Missed	FA
Track 1	0.7548	0.1609	0.0643	0.0200
Track 2	0.2209	0.7548	0.0174	0.0070

Table 14.8: Tracks' Purity with GDA based on Dempster-Shafer Theory (two crossing targets).

	Obs. 1	Obs. 2	Obs. 3	Obs. 4	Missed	FA
Track 1	0.5874	0.2679	0.1211	0.0174	0.0016	0.0047
Track 2	0.2511	0.5489	0.1268	0.0700	0.0011	0.0021
Track 3	0.1216	0.1058	0.5926	0.1742	0.0021	0.0037
Track 4	0.0374	0.0711	0.1505	0.6563	0.0005	0.0042

Table 14.9: Tracks' Purity with GDA based on Dempster-Shafer Theory (four closely spaced targets).

14.7 Comparative analysis of the results

It is evident from the simulation results presented in previous sections, that in general the incorporated advanced concept of generalized data association leads to improving of the tracks' maintenance performance especially in complicated situations (closely spaced and/or crossing targets in clutter). It influenced over the obtained tracks' purity results. In the same time one can see, that the tracks' purity in case of using Dezert-Smarandache theory increases in comparison with the obtained one via Dempster-Shafer theory. Analysing all the obstacles making these simulations, it can be underlined that :

- Dezert-Smarandache theory makes possible to analyze, process and utilize flexibly all the paradoxical information - case, which is peculiar to the problem of multiple target tracking in clutter, when the conflicts between the bodies of evidence (tracks' attribute histories and corresponding attribute measurements) often become high and critical. That way it contributes to a better understanding of the overall tracking situation and to producing an adequate decision. Processing the paradoxes (propositions, which are more specific than the others in the hyper-power set), the estimated entropy in the confirmed (via the right track-observation association) tracks' attribute histories decreases during the consecutive scans. It can be seen on the last figure 14.8, where the Pignistic entropy (i.e the Shannon entropy based on pignistic probabilities derived from the resulting belief mass [15, 11]) is estimated in the frame of $\Theta_1 = \{\text{Very Small (VS), Small (S), Big (B)}\}$ and the corresponding hyper-power set D^{Θ_1} (blue color curve on the top subfigure). Simulation steps show, that source of evidence here is a hybrid one - paradoxical and uncertain. In the same time the entropy of the track's attribute history, described in the second frame $\Theta_2 = \{\text{False Alarm (FA), Fighter (F), Cargo (C)}\}$ (red color curve on the bottom subfigure) increases. It can be explained with the applied here hybrid DSm model $\mathcal{M}_1(\Theta_2)$, built by introducing the exclusivity constraints, imposed by the real life requirements (section 14.3.2.2). The obtained that way model corresponds actually to Shafer's model, which is a particular case of hybrid DSm model (the most constrained one). Therefore, while the corresponding sets in D^{Θ_1} are usually non empty, because of the exclusivity constraints,

in the second frame Θ_2 , the hyper-power set is reduced to:

$$D_{\mathcal{M}_1}^{\Theta_2} = \{\emptyset, FA, F, C, FA \cup F, FA \cup C, F \cup C, FA \cup F \cup C\}$$

So, it is obvious, in that frame, the track's attribute history represents uncertain source of information. Here the entropy increases with the uncertainty during the consecutive scans, because all the masses assigned to the empty sets in D^{Θ_2} are transferred to the non-empty sets, in our case actually to the uncertainty.

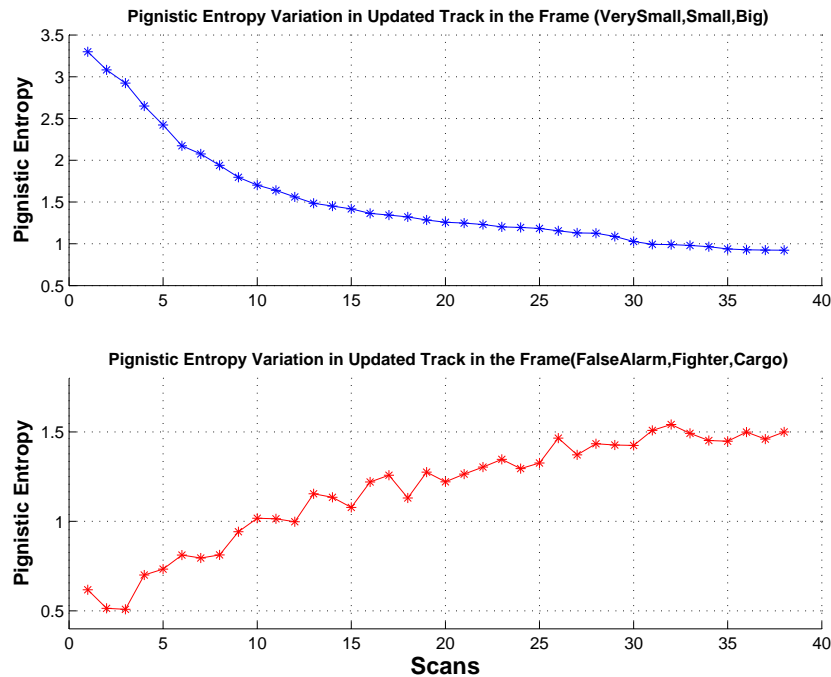


Figure 14.8: Variation of Pignistic Entropy in Track's Attribute History in the two frames Θ_1 and Θ_2

- Because of the Swerling type modelling, the observations for False Alarms, Fighter and Cargo are too much mixed. That fact causes some conflicts between general basic beliefs assignments of the described bodies of evidence. When the conflict becomes unity, it leads to indefiniteness in Dempster's rule of combination and consequently the fusion process can not be realized. From the other side, if the received modeled measurement leads to track's attribute update, in which the unity is assigned to some particular elementary hypothesis, after that point, the combinational rule of Dempster becomes indifferent to any other measurements in the next scans. It means the track's attribute history remains the same, regardless of the received observations. It naturally leads to non coherent and non adequate decisions according to the right observation-to-tracks associations.

14.8 Conclusions

In this work an approach for target tracking, which incorporates the advanced concept of generalized data (kinematics and attribute) association is presented. The realized algorithm is based on Global Nearest Neighbour-like approach and uses Munkres algorithm to resolve the generalized association matrix. The principles of Dezert-Smarandache theory of plausible and paradoxical reasoning to utilize attribute data are applied. Especially the new general hybrid DS_m rule of combination is used to deal with particular integrity constraints associated with some elements of the free distributive lattice. A comparison with the corresponding results, obtained via Dempster-Shafer theory is made. It is proven, that Dempster-Shafer theory is well suited for representing uncertainty, but only in the cases of low conflicts between the bodies of evidence, while Dezert-Smarandache theory contributes to improvement of track maintenance performance in complicated situations (crossing and/or closely spaced targets), assuring a flexible and coherent decision-making, when kinematics data are insufficient to provide the proper decisions.

14.9 References

- [1] Angelova D., Vassileva B., Semerdjiev Tz., *Monte Carlo-based Filter for Target Tracking with Feature Measurement*, Proceedings of the Fifth International Conference on Information Fusion, July 8-11, Annapolis, Maryland, USA, pp. 1499-1505, 2002.
- [2] Bar-Shalom Y., *Multitarget-Multisensor Tracking: Advanced Applications*, Artech House, 1990.
- [3] Bar-Shalom Y., Fortmann T., *Tracking and Data Association*, Academic Press, 1988.
- [4] Bar-Shalom Y., Li X.-R., *Estimation and Tracking : Principles, Techniques and software*, Artech House, 1993.
- [5] Bar-Shalom Y., Li X.-R., *Multitarget-multisensor tracking: Principles and techniques*, YBS, 1995.
- [6] Bar-Shalom Y., Kirubarajan T., Gokberk C., *Classification-Aided Sliding-Window MHT: Solution with Multidimensional Assignment*, ESP Lab, University of Connecticut (Presentation Slides HT Workshop: A Tribute to Sam Blackman, San Diego, CA, May 2003 /May 20, 2003).
- [7] Blackman S., *Multitarget tracking with Radar Applications*, Artech House, 1986.
- [8] Blackman S., Popoli R., *Design and Analysis of Modern Tracking Systems*, Artech House, 1999.
- [9] Bojilov, L.V., *An improved version of a Multiple Targets Tracking Algorithm*, Information & Security, An International Journal, vol. 9, 2002, pp. 130-140.
- [10] Bourgeois F., Lassalle J.C., *An Extension of the Munkres Algorithm for the Assignment Problem to Rectangular Matrices*, Communications of the ACM, Vol.14, Dec.1971, pp.802-806.

- [11] Dezert J., Smarandache F., Daniel M., *The Generalized Pignistic Transformation*, Proceedings of Fusion 2004, Stockholm, Sweden, June 28th-July 1th, 2004.
- [12] Murty K.G., *An Algorithm for Ranking All the Assignment in Order of Increasing Cost*, Operations Research 16, pp. 682-687, 1968.
- [13] Popp R.L., Pattipati K.R., Bar-Shalom Y., *Dynamically Adaptable m-Best 2-D Assignment Algorithm and Multilevel Parallelization*, IEEE Trans.on AES, Vol.35, No.4, Oct.1999.
- [14] Mendel J.M., *Fuzzy Logic Systems for EGINEERING: A Tutorial*, Proceedings of the IEEE, March 1995, pp.345-377.
- [15] Tchamova A., Dezert J., Semerdjiev Tz., Konstantinova P., *Target Tracking with Generalized Data Association based on the General DSm Rule of Combination*, Proceedings of Fusion 2004, Stockholm, Sweden, June 28th-July 1th, 2004.
- [16] Watson G., Blair W.D., *Benchmark Problem for Radar Resource Allocation and Tracking Maneuvering Targets in the presence of ECM*, Technical Report NSWCDD/TR-96/10, 1996.
- [17] Zhou B., Bose N.K., *Multitarget Tracking in Clutter: Fast Algorithms for Data Association*, IEEE Trans. on Aerospace and Electronic Systems, vol.29, No 2, pp. 352-363, April 1993.